Scanning Tunneling Study of the Assembly of Octa- and Tetraruthenium Supermolecules on Graphite

Dong-Lin Shieh,[a] Kom-Bei Shiu,[a] and Jong-Liang Lin*[a]

Keywords: Supermolecular chemistry / Scanning tunneling microscopy / Graphite / Ruthenium

Surface layer structures of $[\{Ru_2(CO)_4(PMe_3)_2\}(\mu\text{-}O_2CCO_2)]_4$ and $[\{Ru_2(CO)_4(PMe_3)_2\}(\mu\text{-}O_2CCH_2CO_2)]_2$ with $[Ru_2(CO)_4(PMe_3)_2]$ building blocks *cis*-ligated by either O_2CCO_2 or $O_2CCH_2CO_2$ on highly oriented pyrolytic graphite (HOPG) have been investigated by scanning tunneling microscopy and spectroscopy. STM images of well-ordered assemblies of these two molecules with molecular or submolecular resolution were obtained. These two molecules can adopt an orientation with their Ru–Ru bonds parallel or perpendicular to the substrate surface forming ordered 2D-arrays with different layer structures and tunneling spectra.

Introduction

The design and applications of unique molecular structures containing special functional units, such as rigid *cis*-bridge transition-metal macrocycles, are major subjects of supermolecular chemistry. An ordered arrangement of supermolecules with rigid macrocyclic structures on surfaces or in their film states is of interest in producing nanoscale devices. Thin-film materials based on tetrametallic squares have been preliminarily proven to show the properties of nanoscale porosity, size-selective transport, and molecular or ionic sensing.[1−3] As an example, it has been reported that the bridge-ligated Re/Pd square cationic complexes, prepared by the reaction of $Re(CO)_3Cl(4,4'\text{-bpy})_2$ and $Pd(dppp)(triflate)_2$, show photoluminescent characteristics which can be used for ClO_4^- anion sensing.[1] However, to date we know of no reported surface structure investigations of either a monolayer or a thin film of rigid superstructures of bridged transition metals.

In the present work we investigate the two dimensional (2D) structures of $[\{Ru_2(CO)_4(PMe_3)_2\}(\mu\text{-}O_2CCO_2)]_4$ (**1**) and $[\{Ru_2(CO)_4(PMe_3)_2\}(\mu\text{-}O_2CCH_2CO_2)]_2$ (**2**) as the first model for supermolecules based on dimetal building units coordinated by *cis*-bridging ligands on HOPG using scanning tunneling microscopy. Figure 1 shows the molecular structures of **1** and **2**. Molecule **1** has an octametallic square shape with four nominally equivalent corner components containing dimetal $[Ru_2(CO)_4(PMe_3)_2]$ building units. Molecule **2** is a molecular loop with two nominally equivalent building blocks. Their crystal structures have been well-characterized by X-ray crystallography.[4] The unique shapes and known dimensions of these molecules allow for the submolecular analysis of the measured STM images. Supermolecules based on dimetal building units can contain various organic ligands that control properties such as solubility, pore size, and electrochemical activity.[5] Furthermore, the spectroscopic and magnetic properties of the dimetal units can be varied for diversified applications.

[a] Department of Chemistry, National Cheng Kung University
1, Ta Hsueh Road, Tainan, Taiwan 701, Republic of China
Fax: (internat.) + 886-6-2740552
E-mail: jonglin@mail.ncku.edu.tw

Results and Discussion

Our scanning tunneling results of $[\{Ru_2(CO)_4(PMe_3)_2\}(\mu\text{-}O_2CCO_2)]_4$ are shown in Figures 2 and 3, and of $[\{Ru_2(CO)_4(PMe_3)_2\}(\mu\text{-}O_2CCH_2CO_2)]_2$ in Figures 4 and 5. Figure 2 (a) shows a 1000×1000 nm^2 STM image with a step separating two terraces after deposition of **1** on the HOPG. The tunneling image and spectrum obtained around point A in the lower area (the dark terrace) is similar to those of a clean graphite surface. Therefore, the dark terrace is attributed to an uncovered area of the graphite surface. Figure 2 (b) shows the STM image recorded at point B on the bright terrace. In this image, the bright lobes form an ordered array and have the same size and tunneling characteristics, suggesting that they are caused by the same molecular or submolecular groups. In Figure 2 (b), the rows of bright lobes along directions C and D have an included angle of $93 \pm 2°$. The distance between two neighboring lobes in both directions is 6.8 ± 0.2 Å. The geometric characteristics of the STM image corresponds to the angle of Ru4−Ru1−Ru8 (92.5°) and the Ru···Ru distance of Ru1−Ru4 or Ru1−Ru8 (6.9 Å) of **1** as shown in Figure 1.

As molecules of **1** are adsorbed with their 2.7 Å Ru−Ru bonds of $[Ru_2(CO)_4(PMe_3)_2]$ building units perpendicular to the HOPG surface, that is, with the PMe_3 groups pointing either toward or away from the HOPG surface; the adsorbed molecular orientation explains the observed

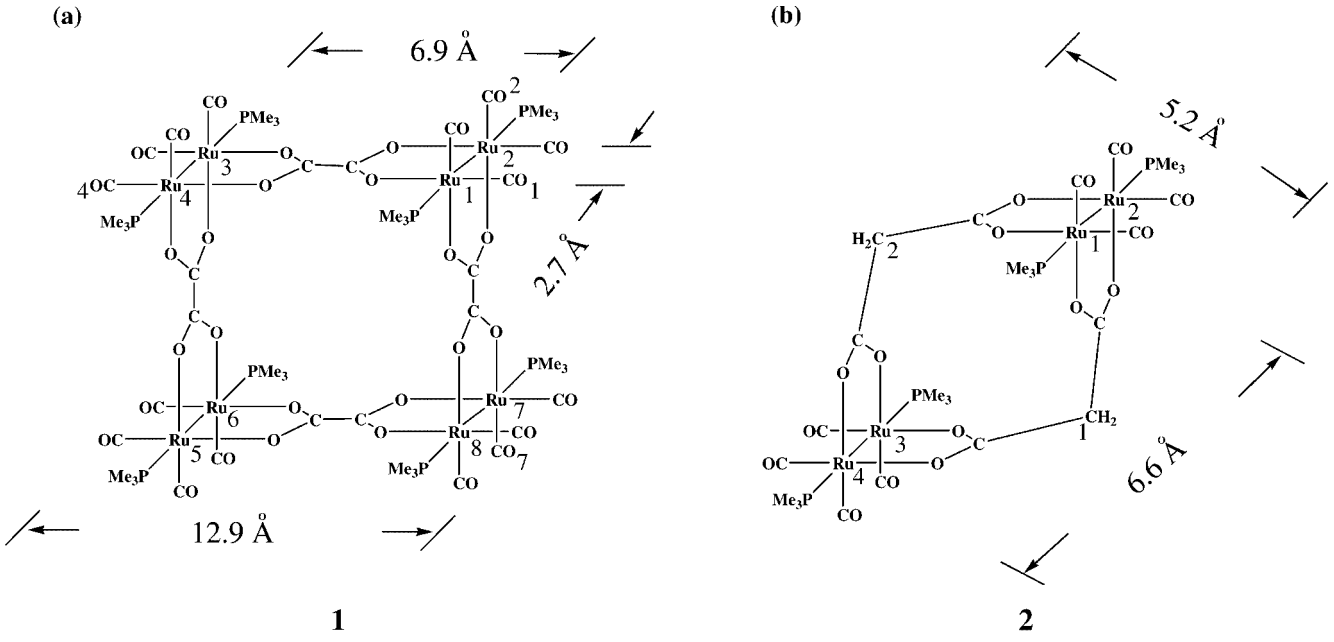

Figure 1. (a) Molecular structure of $[\{Ru_2(CO)_4(PMe_3)_2\}(\mu\text{-}O_2CCO_2)]_4$; the shape of this molecule is close to a square, with four approximately equivalent $[Ru_2(CO)_4(PMe_3)_2]$ corner components; (b) molecular structure of $[\{Ru_2(CO)_4(PMe_3)_2\}(\mu\text{-}O_2CCH_2CO_2)]_2$

distance and angle of the neighboring lobes exactly. The four lobes connected by the square shown in Figure 2 (b) corresponds to a molecule of **1**. Each lobe represents the submolecular image of one corner component, that is, one $[Ru_2(CO)_4(PMe_3)_2]$ unit of **1**. We were able to record a well-ordered 2D domain of approximately 35 × 35 nm^2 at submolecular resolution. Figure 2 (c) shows the proposed molecular adsorption orientation, as well as the 2D assembly of **1** that matches the observed STM image. This layer structure has a surface unit cell of 13.6 × 13.6 Å^2 with a 93° included angle. The size of the unit cell is slightly larger than that of a unit of **1** [O1−O4 = O2−O7 = 12.9 Å as shown in Figure 1 (a)]; that is, the surface molecules are closely packed together.

This packing characteristic has been observed in the previous STM investigation of the $(Co_4L_4)(AsF_6)_8$ layer on HOPG [L = 4,6-bis(2′,2′′-bipyridyl-6-yl)pyrimidine].[6,7] The monolayer has a periodicity of 25 × 24 Å^2, which corresponds to the size of the Co_4L_4 complex ion with a metal grid unit as well. Figure 2 (d) contains the line profiles taken along the directions of C and D shown in Figure 2 (b); the corrugation is approximately 2.2 Å in both cases. Figure 2 (e) compares the tunneling spectra recorded for the area covered by **1** (similar I-V curves are recorded when the tip is positioned on the peaks and valleys of the corrugation) and for a clean graphite surface. The close packing of the bright lobes [c.a. 6.8 Å between two neighboring lobes, Figure 2 (b)] for **1** excludes the possibility that the adsorbed molecules of **1** adopt an orientation where the Ru−Ru bonds (Ru1−Ru2, Ru3−Ru4, Ru5−Ru6, and Ru7−Ru8) are approximately parallel to the HOPG surface [see Figure 1 (a)], because the distance from the H atoms of a PMe_3 group to those of the opposite PMe_3 group in the same corner unit $[Ru_2(CO)_4(PMe_3)_2]$ is approximately 11.5 Å. Taking the van der Waals radius into account, if the adsorbed molecules of **1** on the HOPG have this orientation, the length between two neighboring bright lobes in either the C or D direction should be larger than 11.5 Å [Figure 2 (b)]. Interestingly, an adsorption orientation with the Ru−Ru bonds approximately parallel to the surface is also observed (Figure 3).

Figure 3 (a) shows another STM image (400 × 400 nm^2), with a step separating two terraces, after deposition of **1** on the HOPG. The dark terrace is attributed to the uncovered area of the graphite surface based on the tunneling images and spectra taken in this area. Figure 3 (b) shows the STM image recorded at point A on the bright terrace. In Figure 3 (b) the size of the bright lobes (c.a. 12.8 × 11.6 Å^2) is about four times that found in Figure 2 (b), and corresponds to the size of a molecule of **1** as shown in Figure 3 (c); implying that each bright lobe in Figure 3 (b) represents a molecule of **1**. In other words, this matched dimension implies that **1** adopts an orientation where the four Ru−Ru bonds are approximately parallel to the HOPG surface. Note that the molecular adsorption orientation in this case is perpendicular to that shown in Figure 2 (c). The ordered array of the bright lobes in Figure 3 (b) has a unit cell of 13.7 ± 0.2 × 14.7 ± 0.2 Å^2 with an included angle of 120 ± 2°. Figure 3 (d) shows the proposed molecular adsorption orientation and the 2D assembly of **1** that matches the observed STM image of Figure 3 (b) according to the size of the bright lobes and the unit cell. Although the included angle of 120 ± 2° [i.e. approximately hexagonal symmetry, Figure 3 (b)] may indicate the superperiodic pattern of a bare HOPG surface, other tunneling features are not consistent with this argument. First, in Figure 3 (b) the corru-

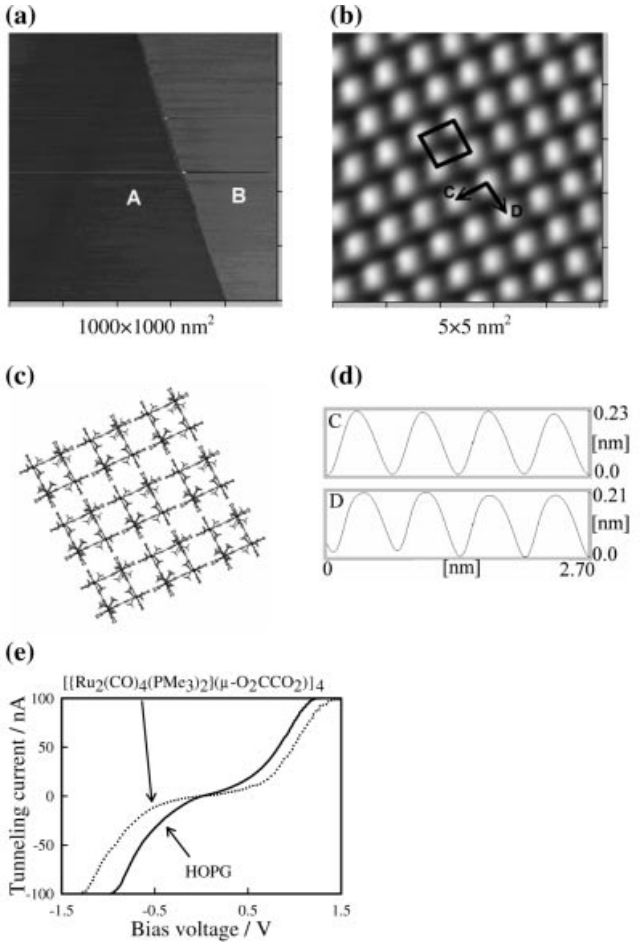

Figure 2. (a) STM image of 1000 × 1000 nm² with a step separating a bright terrace representing a $[\{Ru_2(CO)_4(PMe_3)_2\}(\mu\text{-}O_2CCO_2)]_4$-covered area and a dark terrace representing uncovered area of HOPG; (b) high-resolution STM image of the $[\{Ru_2(CO)_4(PMe_3)_2\}(\mu\text{-}O_2CCO_2)]_4$-covered area on HOPG; (c) proposed 2D array that matches the STM image; (d) line profiles in the directions of C and D; (e) comparison of tunneling spectra of the $[\{Ru_2(CO)_4(PMe_3)_2\}(\mu\text{-}O_2CCO_2)]_4$-covered surface and a bare HOPG surface. V = 0.1 V and I = 0.25 nA were used to record the STM images

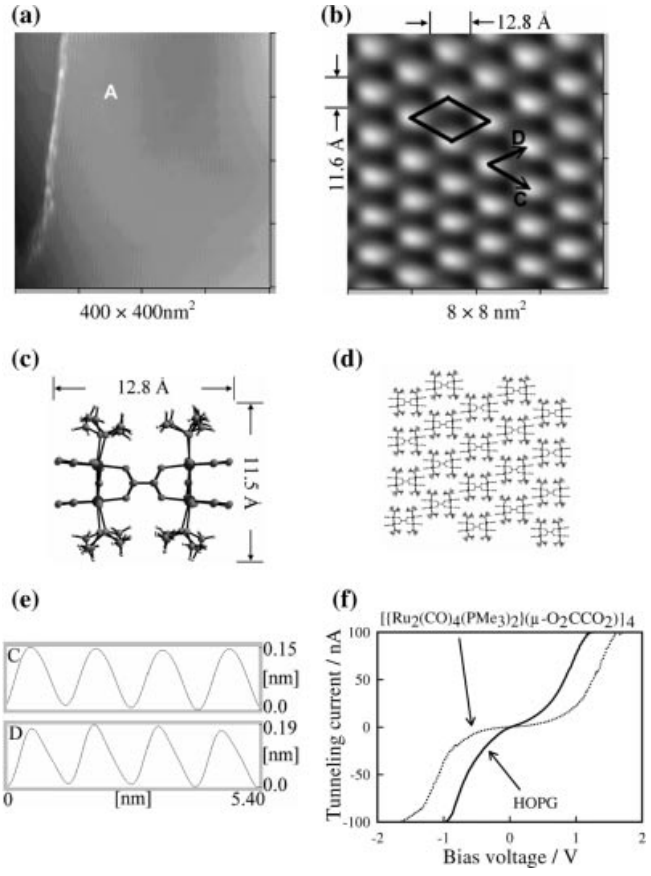

Figure 3. (a) STM image of 400 × 400 nm² with a step separating a bright terrace representing a $[\{Ru_2(CO)_4(PMe_3)_2\}(\mu\text{-}O_2CCO_2)]_4$-covered area and a dark terrace representing uncovered area of HOPG; (b) high-resolution STM image of the $[\{Ru_2(CO)_4(PMe_3)_2\}(\mu\text{-}O_2CCO_2)]_4$-covered area on HOPG; (c) $[\{Ru_2(CO)_4(PMe_3)_2\}(\mu\text{-}O_2CCO_2)]_4$ structure with the indicated dimensions similar to those of the bright lobes in the STM image; (d) proposed 2D array that matches the STM image; (e) line profiles in the directions of C and D; (f) comparison of tunneling spectra of the $[\{Ru_2(CO)_4(PMe_3)_2\}(\mu\text{-}O_2CCO_2)]_4$-covered surface and a bare HOPG surface; V = 0.1 V and I = 0.25 nA were used to record the STM images

gations in the C and D directions [these are approximately 0.17 nm, as shown in Figure 3 (e)] are much smaller than the approximate 1−1.5 nm reported for HOPG superlattices.[8,9] Second, no graphite atomic fringes were observed in Figure 3 (b), which were also observed in the STM images of HOPG superlattices.[8,9] Figure 3 (f) shows the tunneling spectrum of Figure 3 (b).

Figure 4 (a) shows the STM image of a covered area comprising molecules of **2** on the HOPG. The rows of bright lobes along directions C and D have an included angle of 110 ± 2°. The distance between two neighboring lobes in either direction is 6.8 ± 0.2 Å. This length corresponds to 6.6 Å between the equivalent parts of the $[Ru_2(CO)_4(PMe_3)_2]$ unit, as shown in Figure 1 (b), suggesting that the bright lobes in Figure 4 (a) are due to $[Ru_2(CO)_4(PMe_3)_2]$ units. Note that the distance between the two CH_2 groups of **2** is only 5.2 Å, which is approximately 1.6 Å less than the distance between two neighboring lobes in Figure 4 (a). Furthermore, the sizes of the bright lobes in Figure 2 (b) for **1** and in Figure 4 (a) for **2** are similar. Therefore, the bright lobes in Figure 4 (a) are not attributed to the CH_2 groups of **2**, but rather to the $[Ru_2(CO)_4(PMe_3)_2]$ units, and as a result, we propose that **2** is adsorbed in such a way that the PMe_3 groups of $[Ru_2(CO)_4(PMe_3)_2]$ point either toward or away from the HOPG surface. Because each bright lobe in Figure 4 (a) corresponds to a $[Ru_2(CO)_4(PMe_3)_2]$ unit, there are three possible 2D assemblies [as shown in Figure 4 (b)] that match the observed STM image. The three different 2D layer structures have surface unit cells of 12.1 × 15.8 Å² with an 87° included angle, 12.1 × 8.0 Å² with a 99° angle, and 13.5 × 8.0 Å² with an 124° angle. Note that the three different layer structures displayed next to each other in Figure 4 (b) do not mean that they co-exist in the STM sampling area of Figure 4 (a). Figure 4 (c) shows the line profiles in the directions of C and D of Figure 4 (a). Figure 4 (d) compares the tunneling spectra recorded for the layer of **2** and

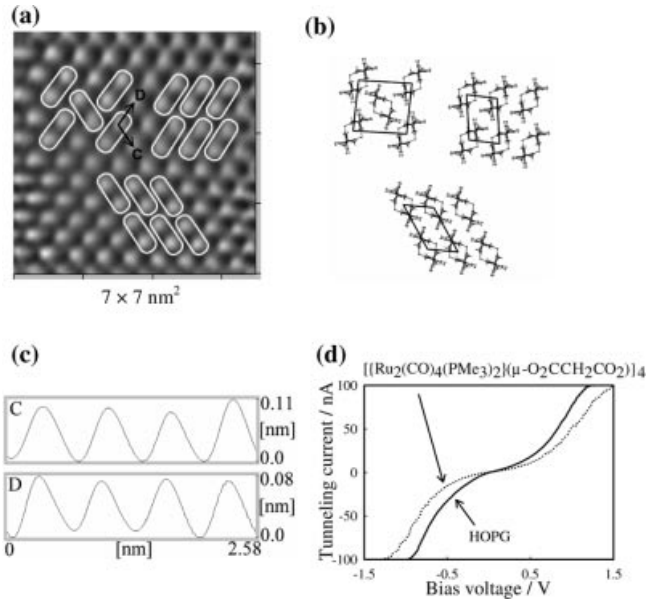

Figure 4. (a) STM image of a $[\{Ru_2(CO)_4(PMe_3)_2\}(\mu\text{-}O_2CCH_2CO_2)]_2$-covered area on HOPG; (b) proposed three possible 2D arrays that match the STM image; (c) line profiles in the directions of C and D; (d) comparison of tunneling spectra of the $[\{Ru_2(CO)_4(PMe_3)_2\}(\mu\text{-}O_2CCH_2CO_2)]_2$-covered surface and a bare HOPG surface; $V = 0.05$ V and $I = 0.34$ nA were used to record the STM image

a clean HOPG surface. Note that because the molecular adsorption orientations of **1** and **2** are similar [Figure 2 (c) and Figure 4 (b), respectively], that is, with the PMe_3 groups pointing either toward or away from the HOPG surface, the tunneling spectra of **1** and **2** are also similar [Figure 2 (e) and Figure 4 (d), respectively].

Figure 5 (a) shows another observed STM image of **2**, consisting of an ordered array of bright lobes with an approximate size of 11.5×10.2 Å^2. Similar dimensions of a molecule of **2** are shown in Figure 5 (b). This similarity suggests that each lobe in Figure 5 (a) corresponds to a molecule of **2** adsorbed with the two Ru−Ru bonds approximately parallel to the HOPG surface. Note that the orientation of the surface molecules in this case is perpendicular to that shown in Figure 4 (b). The ordered array of the bright lobes in Figure 5 (a) has a unit cell of $11.3 \pm 0.2 \times 13.8 \pm 0.2$ Å^2 with an included angle of $83 \pm 3°$. Figure 5 (c) shows the proposed molecular adsorption orientation and the 2D assembly of molecules of **2** that match the STM image of Figure 5 (a). Figure 5 (d) shows the line profiles in the directions of C and D of Figure 5 (a). Figure 5 (e) compares the tunneling spectra recorded for a layer of **2** with a clean HOPG surface.

Conclusion

In summary, we find that on the HOPG the studied octa- and tetraruthenium supermolecules can both adopt an orientation with their Ru−Ru bonds parallel or perpendicular to the substrate surface, forming ordered 2D arrays with different layer structures and tunneling spectra. We

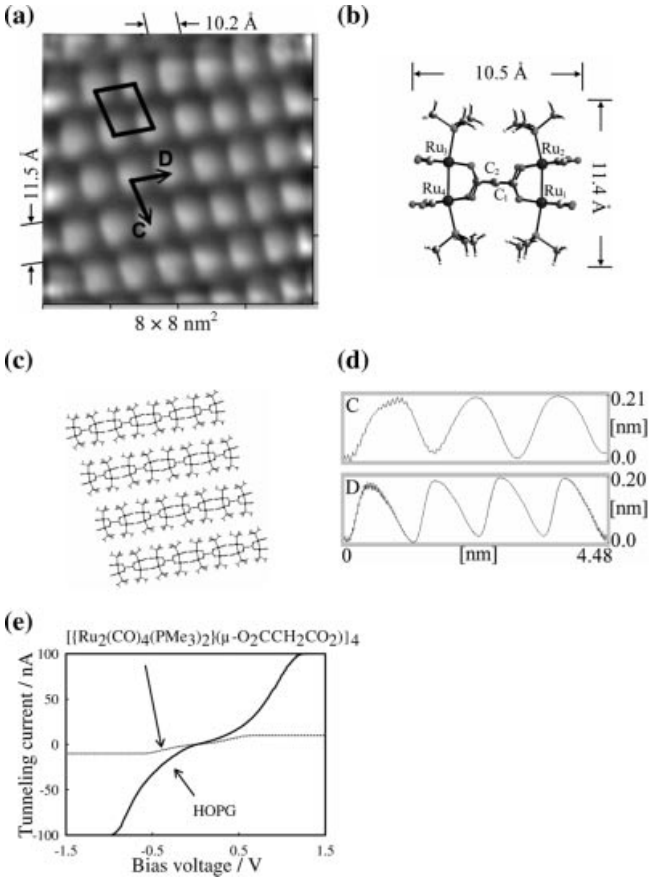

Figure 5. (a) STM image of a $[\{Ru_2(CO)_4(PMe_3)_2\}(\mu\text{-}O_2CCH_2CO_2)]_2$-covered area on HOPG; (b) $[\{Ru_2(CO)_4(PMe_3)_2\}(\mu\text{-}O_2CCH_2CO_2)]_2$ structure with the indicated dimensions similar to those of the bright lobes in the STM image; (c) proposed 2D array that matches the STM image; (d) line profiles in the directions of C and D; (e) comparison of tunneling spectra of the $[\{Ru_2(CO)_4(PMe_3)_2\}(\mu\text{-}O_2CCH_2CO_2)]_2$-covered surface and a bare HOPG surface. $V = 0.05$ V and $I = 0.34$ nA were used to record the STM image

compare, with the aid of the software *Diamond*, the observed 2D structures of the molecules of **1** and **2** on the HOPG to the crystallographic planes of 3D structures of **1** and **2** and find no similar cases that simultaneously have both the same dimensions of the unit cells and the same molecular orientations as those in Figure 2 (c), 3 (d), 4 (b), or 5 (c). This result indicates the influence of the HOPG surface on the 2D assemblies of molecules of **1** and **2**.

Experimental Section

General: $[\{Ru_2(CO)_4(PMe_3)_2\}(\mu\text{-}O_2CCO_2)]_4$ (**1**) and $[\{Ru_2(CO)_4(PMe_3)_2\}(\mu\text{-}O_2CCH_2CO_2)]_2$ (**2**) were synthesized through the reactions of freshly prepared $Ru_3(CO)_{12}$, oxalic acid, and PMe_3 in THF according to a procedure previously described.[5] In the preparation of adsorption films of **1** and **2** on HOPG, a droplet of **1** (0.01 M) or **2** (0.03 M) in CH_2Cl_2 was deposited onto a freshly cleaved surface of HOPG (ZYB quality). The CH_2Cl_2 was allowed to vaporize before STM images were recorded (Seiko Instruments, SPA 400) at constant current mode under ambient conditions. The film systems were stable, permitting repeated scans within several months of the

investigation period. Electrochemically etched W tips were used for the STM study.

Acknowledgments

We gratefully acknowledge the support of the National Science Council of the Republic of China (NSC 92-2113-M-006-016).

[1] R. V. Slone, D. I. Yoon, R. M. Calhoun, J. T. Hupp, *J. Am. Chem. Soc.* **1995**, *117*, 11813−11814.
[2] R. V. Slone, K. D. Benkstein, S. B'elanger, J. T. Hupp, I. A. Guzei, A. L. Rheingold, *Coord. Chem. Rev.* **1998**, *171*, 221−243.
[3] S. B'elanger, J. T. Hupp, C. L. Stern, R. V. Slone, D. F. Watson, T. G. Carrell, *J. Am. Chem. Soc.* **1999**, *121*, 557−563.
[4] K.-B. Shiu, H.-C. Lee, G.-H. Lee, Y. Wang, *Organometallics* **2002**, *21*, 4013−4016.
[5] F. A. Cotton, C. Lin, C. A. Murillo, *Acc. Chem. Res.* **2001**, *34*, 759−771.
[6] A. Semenov, J. P. Spatz, M. Möller, J.-M. Lehn, B. Sell, D. Schubert, C. H. Weidl, U. S. Schubert, *Angew. Chem. Int. Ed.* **1999**, *38*, 2547−2550.
[7] A. Semenov, J. P. Spatz, J.-M. Lehn, C. H. Weidl, U. S. Schubert, M. Möller, *Appl. Surf. Sci.* **1999**, *144−145*, 456−460.
[8] M. Kuwabara, D. R. Clarke, D. A. Smith, *Appl. Phys. Lett.* **1990**, *56*, 2396−2398.
[9] J. Xhie, K. Sattler, M. Ge, N. Venkateswaran, *Phys. Rev. B* **1993**, *47*, 15835−15841.

Received November 24, 2003

